NANO LETTERS

Letter

pubs.acs.org/NanoLett

Pointwise Plucking of Suspended Carbon Nanotubes

Jun Luo,*[,†,‡,§] Wengen Ouyang,[§,∥] Xiaopei Li,[†] Zhong Jin,[⊥] Leijing Yang,[¶] Changqing Chen,[§,∥] Jin Zhang,[⊥] Yan Li,[⊥] Jamie H. Warner,[‡] Lian-mao Peng,[¶] Quanshui Zheng,[§,∥] and Jing Zhu*[,†,§]

[†]Beijing National Center for Electron Microscopy, The State Key Laboratory of New Ceramics and Fine Processing and Laboratory of Advanced Materials, Department of Materials Science and Engineering, Tsinghua University, Beijing 100084, China

[‡]Department of Materials, University of Oxford, Parks Road, Oxford OX1 3PH, United Kingdom

[§]Center for Nano and Micro Mechanics and [∥]Department of Engineering Mechanics, Tsinghua University, Beijing 100084, China

[⊥]College of Chemistry and Molecular Engineering and [¶]Department of Electronics, Peking University, Beijing 100871, China

Supporting Information

ABSTRACT: Vibration of nanotubes/wires is significant for fundamental and applied researches. However, it remains challenging to control the vibration with point-level precision. Herein, individual suspended carbon nanotubes are plucked point by point to vibrate in scanning electron microscope with the electron beam as a nanoscale pointer. The vibration is directly imaged, and its images fit well with simulations from the plucking mechanism. This demonstrates a new way to manipulate the nanotube vibration with unprecedented precision.

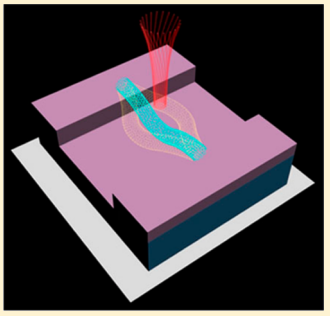

KEYWORDS: *Carbon nanotube, plucking, pointwise, vibration, point-level precision, electron beam*

Vibration of a macroscopic beam or string is ubiquitous in nature and has been employed in research, arts, industry, and domesticity.[1−4] Advances in nanoscience and nanotechnology have enabled forces to be applied collectively on the entirety of a suspended carbon nanotube (CNT), driving its vibrations at the mesoscopic scale.[5−12] The CNT vibrations have been widely put into scientific studies and technological applications, including adsorption analysis at the single-atom level,[5] coupling between single-electron tunneling and mechanical motion,[6−8] and ultrasensitive force, mass, and magnetism detections.[9−12] However, it is still highly challenging and difficult to focus a force on a local segment or point of a CNT and control accurately its motion and position. Plucking CNTs to vibrate by discrete point loading is one way of achieving the control with point-level precision but has not been realized so far in nanomaterials, although its macroscopic counterpart has been extensively studied and utilized in bridge construction[2,3] and in musical string instruments.[4]

In this Letter, we demonstrate that individual suspended CNTs can be plucked point by point to vibrate in situ in a scanning electron microscope (SEM), where the electron beam (e-beam) worked as a virtual nanoscale pointer and a force was focused and applied on discrete points of the CNTs under the guide of the e-beam. The vibration was directly imaged, and its images fit well with simulations from the plucking mechanism. The CNT Young's modulus was extracted to be 1.23 TPa, which is in good agreement with data previously reported.[13,14] This presents a new way to accurately manipulate the vibrational characteristics of nanotubes/wires and opens the pathway toward developing novel acoustic, mechanical, and electromechanical nanodevices with high precision.

Our CNTs were produced by chemical vapor deposition,[15] lay horizontally on a Si substrate with oxide surface, and were characterized to be single-walled by Raman spectra and transmission electron microscope (TEM).[15,16] Trenches of 3.4 μm width and 580 nm depth existed in the oxide surface, and some CNTs crossed over them, such as the one (CNT #1) shown in Figure 1a. SEM images cannot be used to measure the real diameter of ultrathin CNTs,[15,16] and so we applied atomic force microscopy on the nonsuspended segments of CNT #1 lying on the SiO_2 beside the trench and found that its diameter was 2.4 ± 0.2 nm. The trench bottom below its suspended segment was also covered by an oxide layer of 46 nm thickness. Figure 1b indicates that the suspended length was longer than the distance between the two clamping points and its curvature was vertically downward to the trench bottom. Figure 1c gives the three-dimensional (3D) schematic image for the CNT with the e-beam in SEM.

The e-beam scanned the surfaces of the CNT and the oxide layer point by point with the sequence running from left to right along the y direction and from back to front along the x direction during any SEM imaging process. The oxide layer was insulating and could be charged by the e-beam, which was verified by the experimental observation that the leakage

Received: April 15, 2012
Revised: May 28, 2012
Published: June 13, 2012

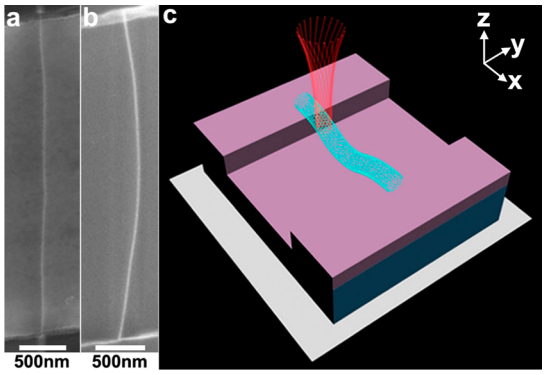

Figure 1. SEM and schematic images of CNT #1 when it was immobile. (a,b) Top-view SEM images of CNT #1 when it was untilted and tilted by 30°, respectively. (c) The 3D schematic image (not to scale) for CNT #1 in SEM, where the red, cyan, magenta, and dark blue icons denote the e-beam, CNT, SiO_2 and Si, respectively.

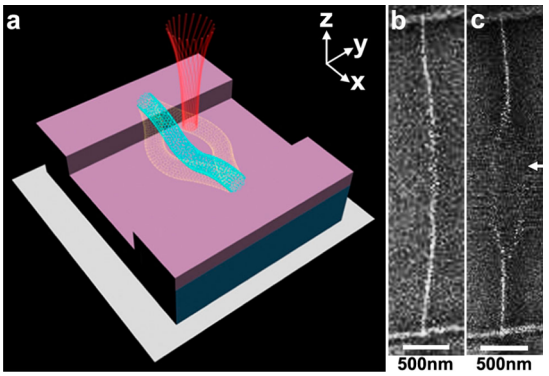

Figure 2. Schematic and SEM images of CNT #1 when it was vibrating. (a) The 3D schematic image for the vibrating CNT, where the yellow icons denote its two shapes at two different moments. (b,c) Top-view SEM images of the CNT in two scanning periods with d_0 = 12.1 and 8.3 nm, respectively. The CNT was kept untilted in its vibration. (b,c) These were cut from two intact SEM images.

current flowing through the oxide layer and the substrate to ground was nonzero and negative when a region on the oxide layer was scanned by the e-beam.[17] The charge in the oxide layer of the substrate must produce an electric field around the CNT. But, the CNT was conductive, grounded,[16] (also see more details in Supporting Information) and so unaffected by the electric field, unless it was charged by the e-beam. The diameter of the e-beam had been indicated to range between 5.0 and 24.6 nm,[16] far smaller than the suspended length of CNT #1. Hence, it was rational to consider an area covered by the e-beam at any given moment as a point. When the e-beam met CNT #1, a point on CNT #1 was irradiated by the e-beam. Some internal electrons in the CNT point were kicked out by the high-energy external electrons in the e-beam and emitted as secondary electrons. Almost at the same time, the external electrons penetrated fast through the CNT point and did not stay within it. Therefore, the CNT point lost some electrons in total and a net positive charge was left on it.[16] This point charge interacted with the electric field produced by the charged oxide layer, generating an electrostatic force on the CNT point. Then the force could cause the CNT to be plucked. The above process implies two points: the e-beam worked as a nanoscale pointer and exposed the CNT point, which was originally "invisible" to the electric field; both the point charge and the charged substrate were necessary for the plucking mechanism.

Initially the electrostatic force and the curved CNT were both in the z plane. If the exposed CNT point was not either of the clamping ones, an in-plane vibration mode would occur. But, the forcing condition easily suffered from small perturbation (such as the small fluctuation of the charge in the substrate), driving the curved CNT to deviate slightly from the z plane. This could induce a moment, causing the CNT to vibrate out of the z plane,[18] as depicted by Figure 2a. As soon as the e-beam left the point, it became uncharged and so "invisible" again to the electric field. Later, when the e-beam met another point on the CNT, the CNT would be plucked again. Accordingly, we could realize plucking the CNT point by point to vibrate, like plucking a string on a guitar with a finger or a beam on a bridge with strong wind. This was confirmed by our experiments and simulations.

First, we used the e-beam with the accelerating voltage of 1 kV to scan an oxide region of 79 μm × 59 μm with CNT #1 at its center for a period. The period is defined as the time taken for the e-beam to complete scanning an intact SEM image consisting of N (y-directional) × M (x-directional) pixels. It equals $N \times M \times t_d$, where t_d (= $100 \times 2^{p-1}$ ns) is the dwell time of the e-beam on each pixel. p is the ranking integer number of the nominal scanning speed. This initial scanning had the parameters of N = 1024, M = 768, and p = 7 and caused the oxide region to be charged. Then, we changed p to 1, fixed it and started to increase the magnification, namely to decrease the pixel size that was inversely proportional to the magnification and denoted by d_0. With the successive decrease of d_0, CNT #1 was observed by SEM to deviate from its original position and to vibrate, as shown in Figure 2b,c (see also Supporting Information Movie 1). d_0 = 12.1 and 8.3 nm in Figure 2b,c, respectively, indicating that the images of the vibrating CNT corresponding to different values of d_0 were different.

Figure 2b,c shows another three unexpected characteristics: (i) the CNT image in Figure 2c is not continuous and contains gaps, of which one is indicated by the white arrow; (ii) the segments of the suspended CNT close to its ends seemed immobile during the vibration, and Figure 3 gives the percentages of the immobile segments in the total distance between the clamping points during different scanning periods; and (iii) the CNT ends seemed not to be arcs. All of the above

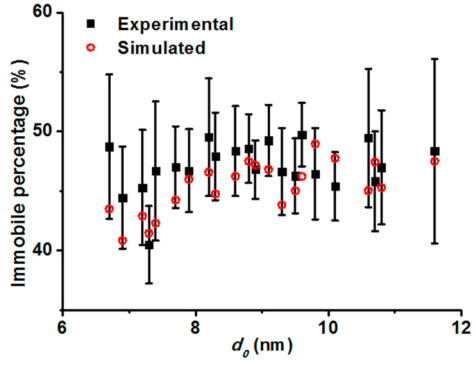

Figure 3. Percentages of the immobile segments of CNT #1 in the total distance between the clamping points during the scanning periods with different values of d_0. The data shown by square and round points are from the experimental and simulated vibration images, respectively. Each error bar is made by standard deviation from six measurements.

dx.doi.org/10.1021/nl301414h | Nano Lett. 2012, 12, 3663−3667

characteristics were also observed on the vibrations of another two CNTs (see Supporting Information Movies 2a, 2b and 3 for CNTs #2 and #3, respectively).

To explore the origin of the above characteristics and the driving mechanism, we analyzed the forcing condition on the CNT. The initially charged oxide region was 79 μm × 59 μm, far larger than the length of the suspended CNT, and so the distribution of the electric field around the CNT suspended length could be considered to be approximately uniform. We observed that the suspended length of CNT #1 was driven to vibrate for 20 s (see Supporting Information Movie 1; after the 20 s vibration, the suspended length partially went out of the SEM view area). This time was far shorter than general time taken for charge in silicon oxides to discharge completely, which had been indicated to be several minutes or longer.[19,20] We used the vibration of CNT #2 with each SEM parameter fixed to check the discharging time of our oxide. This vibration had images similar to those of CNT #1, lasted for more than 1.5 min, and then stopped. Because its SEM parameters were all fixed, the reason to cause its stopping should be only that the charge in the oxide discharged excessively. This implies that the discharging time was longer than 1.5 min, far longer than the observed vibration time of CNT #1. Hence, we considered that during the 20 s vibration of CNT #1 the charging state in the oxide was constant and so the strength of the electric field around CNT #1 was constant. On the basis of the above considerations and the interaction mechanism between e-beam and CNT,[16] we derived that the impulse applied on a point on CNT #1 was proportional to t_d and inversely proportional to d_0, when the e-beam scanned pixels around the CNT point and had overlap with it. The derived expression is as follows (see its derivation detail in Supporting Information)

$$i_t = \frac{S t_d \tau I_b \delta_{CNT} d_{CNT}}{d_0} \tag{1}$$

where i_t is the total impulse applied on the CNT point, S is the strength of the electric field caused by the charge in the oxide, τ is the average lifetime of the elementary charges on the CNT point, I_b is the current of the e-beam, δ_{CNT} is the secondary electron yield of the CNT, and d_{CNT} is the CNT diameter. The reason why we used impulse instead of force is that the interacting time between a CNT point and the e-beam was too short. Equation 1 implies that if d_0 is changed, the impulse and so the vibration image of the CNT will change. This is consistent with the experimental observation that difference exists between Figure 2b,c. Likewise, if t_d, namely p, is changed, the vibration image of the CNT will also change. Experimentally, we changed p from 1 to 2 and found that CNT #1 became totally immobile in SEM and had the same image as that in Figure 1a (see more SEM images in Supporting Information).

We model the CNT as a curved beam suspended over a trench and plucked point by point with the impulse. This is because single-walled CNTs are stiff in both the axial direction and the basal plane[21] and so should be treated as beams.[1,12] According to the out-of-plane vibration equations of a curved beam suspended over a trench,[22,23] we can get the displacement $v^{(k)}(x,t)$ of the CNT along the y direction at the position of x and the time of t after the kth plucking as follows

$$\begin{aligned} v^{(k)}(\xi, t) &= \sum_{n=1}^{\infty} Y_n(\xi)[A_n^{(k)} \cos \Omega' + B_n^{(k)} \sin \Omega'] \cdot \exp(\Omega'') \\ \Omega' &= \Omega_d (t - t_{k-1}) \\ \Omega'' &= -\zeta \Omega_n (t - t_{k-1}) \end{aligned} \tag{2}$$

where $\xi = x/l$, l is the distance between the clamping points, $Y_n(x)$ is the nth principle mode, $A_n^{(k)}$ and $B_n^{(k)}$ are coefficients relevant to i_t, Ω_d and Ω_n are the actual and the nth natural frequencies of the curved CNT, t_{k-1} is the time of the $(k-1)$th plucking, and ζ is the damping ratio. The expressions of Ω_n and Ω_d are given as follows (see those of $Y_n(x)$, $A_n^{(k)}$, $B_n^{(k)}$ and ζ in Supporting Information)

$$\Omega_n = \Omega_{0n}\left[1 - \varepsilon^2 \frac{\pi^2}{2}\left(1 + \alpha_n \frac{2\pi^2}{\lambda_n^4} \frac{GI_\theta}{EI_\xi}\right)\right] \tag{3}$$

$$\varepsilon = \frac{w_{0,\max}}{l}, \quad \alpha_n = -\lambda_n r_n (\lambda_n r_n - 2) \tag{4}$$

$$\Omega_d = \Omega_n \sqrt{1 - 2\zeta^2} \tag{5}$$

where Ω_{0n} is the nth natural frequency of the straight counterpart of the curved CNT, $w_{0,\max}$ is the maximum initial displacement of the CNT in the z direction (in our case $0 < \varepsilon \ll 1$), λ_n is the nth eigenvalue of the equation $\cos\lambda \cdot \cosh\lambda = 1$, r_n is a coefficient (see its expression in Supporting Information), E is the Young's modulus of the CNT, G is the shear modulus of the CNT, and EI_ξ and GI_θ are the bending and torsion stiffnesses of the CNT cross section, respectively. Further, when the vibrating CNT meets the e-beam, the following equation is satisfied

$$v^{(k)}(\eta_k, t_k) = \left(\frac{t_k}{t_d} - kN\right) d_0 \tag{6}$$

where $\eta_k = kd_0$. The right term in eq 6 represents the y-directional position of the e-beam. (See the derivation details of eqs 2−6 in Supporting Information.)

By eqs 1−6 we can get the position of any CNT point and the time when it meets the e-beam and is irradiated by the e-beam. Thus, by drawing points at the meeting positions we can obtain the simulated vibration image of the CNT, because any SEM image of a CNT is composed of the signals from these meeting points in a given period. Figure 4a,b shows the simulated results corresponding to Figure 2b,c, respectively. They fit well with the experimental SEM images. Particularly, the simulated image in Figure 4b contains a gap at the position of the experimental gap in Figure 2c. This matching implies that the experimental gap was caused by the reason that the e-beam did not meet the CNT in the gap zone and so no signals from the CNT were detected by SEM. The reason why the CNT end segments had the image of an immobile line in the vibrations is also relevant to the meeting timing between the e-beam and the CNT. We take the end segment in the yellow box in Figure 4b as an example. Its simulated image is redrawn by red in Figure 4c, whose x- and y-directional scales are the same as those in Figure 4b. Because of the pointwise scanning mode of the e-beam, the end image should be composed of some discrete points, which will be shown later in Figure 4e. Each of the points corresponds to a time when the e-beam met the CNT. The entire shape of the CNT at each meeting time has

dx.doi.org/10.1021/nl301414h | Nano Lett. 2012, 12, 3663−3667

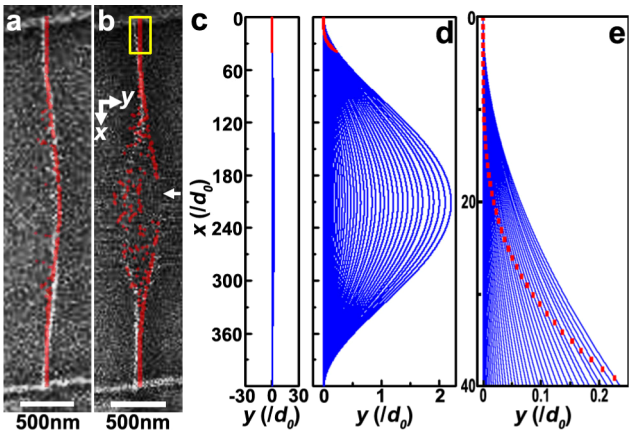

Figure 4. Simulated images and shapes of the vibrating CNT by the plucking mechanism. (a,b) Simulated images corresponding to Figure 2b,c, respectively. They are shown by semitransparent red and superimposed on Figure 2b,c. (c) Simulated end image in the yellow box in (b) and its corresponding simulated entire CNT shapes, where the former and the latter are shown by red and blue, respectively. The *x*- and *y*-directional scales are the same as those in (b). (d) Enlargement of (c) with the *y*-directional scale zoomed in. (e) Further enlargement of the simulated end image and shapes in (d).

been simulated and is shown by a blue line in Figure 4c. Their *y*-directional spacings are so small that they cannot be distinguished. After the *y*-directional scale is zoomed in, the simulated entire CNT shapes can be seen clearly, as depicted in Figure 4d. Figure 4e shows the further enlargement of the end image and shapes. We can see that each blue line represents the entire shape of the CNT at a meeting time, but only one point on each blue line can be met and captured by the e-beam. These captured points compose a seemingly immobile line that is the image of the end. (Likewise, if all of the points captured in the entire SEM imaging process are drawn, we can obtain the entire image in Figure 4b.) The percentages of the immobile segments in the simulated vibration images were measured and found to be close to their experimental counterparts within the error bars, as shown in Figure 3. In addition, Figure 4e indicates that the simulated end image and shapes are all arcs, but their *y*-directional widths are all smaller than the pixel size (d_0). Therefore, the arc characteristic of the CNT end cannot be exhibited in experiments. The SEM images of CNT #1 with p = 2 have been also simulated, and the results are all an immobile line and consistent with the SEM images (see the SEM and simulated images in Supporting Information). The Young's modulus E of the CNT is a crucial parameter in all of the above simulations, and the excellent fitting between the simulated and experimental results gives its value as 1.23 TPa (see more details in Supporting Information). This is in good agreement with the values previously reported.[13,14] It should be noted that eq 2 indicates that multiple principle modes should be considered in the calculations. Actually we considered the first 30 modes, because we found that it was impractical to calculate infinite modes and no detectable difference existed between the results given by the calculations with the first 30 and the first 50 modes.

The consistencies between the simulated and experimental results conclude that we have successfully realized plucking the CNTs point by point to vibrate. This introduces a paradigm to manipulate accurately the vibrations of nanotubes/wires. The manipulation is based on focusing and applying a force not on the entirety but on discrete points of a nanotube. This opens the path to precise control on the motion of nanomaterials and to new device performance for wide applications. Particularly, nanoscale source and focusing technique of e-beam based on individual CNTs have been successfully developed.[24,25] If the pointwise plucking mechanism is integrated with them, it would be promising to develop acoustic, mechanical, or electromechanical nanosystems, such as nanotuner and nanoguitar, with unprecedented precision.

If a suspended CNT is plucked for only one time at any point (except the two clamping points) on it, it can also vibrate. For example, we have calculated the dependence of the *y*-directional vibration amplitude of the central point of CNT #1 on time after the CNT is plucked for one time at the central point. This dependence is shown in Figure 5 and indicates that

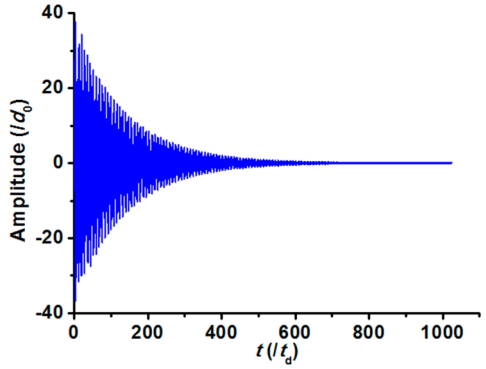

Figure 5. Calculated dependence of the *y*-directional vibration amplitude of the central point of CNT #1 on time after the CNT is plucked for only one time at the central point by the same impulse as that of the multiple plucking.

the nonzero amplitude can persist for more than $600t_d$. The relationship between the vibration and the chirality of a CNT is another interesting issue to explore. We have performed Raman with the lasers of 532 and 633 nm on our CNTs for their chiralities. Some showed Raman signals,[16] but those in this work did not. This should be due to the mismatch between the CNT band structures and the laser excitations.[26] TEM-compatible devices would be an alternative approach for this issue.

■ ASSOCIATED CONTENT

Supporting Information

The movies recording the vibrations of CNTs #1−3 (movies 1 (si_002.avi) and 3 (si_005.avi) are for CNTs #1 and 3, respectively, and movies 2a (si_003.avi) and 2b (si_004.avi) are in succession and for CNT #2), the analysis of the impulse on the CNTs, the mechanical modeling and simulations of the CNTs and their vibration images, and the electrical measurement on the CNTs. This material is available free of charge via the Internet at http://pubs.acs.org.

■ AUTHOR INFORMATION

Corresponding Author

*E-mail: (J.L.) jluo@mail.tsinghua.edu.cn; (J.Z.) jzhu@mail.tsinghua.edu.cn.

Notes

The authors declare no competing financial interest.

■ ACKNOWLEDGMENTS

The authors thank Mr. Lei Yang for drawing the schematic images and Ms. Xiangying Ji, Dr. Andrew A. R. Watt, and Professors Xiqiao Feng and G. Andrew D. Briggs for discussions. This work was supported by National Natural Science Foundation, National 973 Project, NNSF for Young Scholars (51102145), the Foundation for the Author of National Excellent Doctoral Dissertation (201141), and National Program for Thousand Young Talents of China. This work made use of the resources of Beijing National Center for Electron Microscopy.

■ REFERENCES

(1) Weaver Jr., W.; Timoshenko, S. P.; Young, D. H. *Vibration Problems in Engineering*, 5th ed.; John Wiley & Sons: New York, 1990.
(2) Frýba, L. *Dynamics of Railway Bridges*; Thomas Telford: London, 1996.
(3) Gimsing, N. J. *Cable Supported Bridges*; John Wiley & Sons: Chichester, 1997.
(4) King, G. C. *Vibrations and Waves*; John Wiley & Sons: Hoboken, 2009.
(5) Wang, Z. H.; Wei, J.; Morse, P.; Dash, J. G.; Vilches, O. E.; Cobden, D. H. *Science* **2010**, *327*, 552.
(6) Steele, G. A.; Hüttel, A. K.; Witkamp, B.; Poot, M.; Meerwaldt, H. B.; Kouwenhoven, L. P.; van der Zant, H. S. J. *Science* **2009**, *325*, 1103.
(7) Lassagne, B.; Tarakanov, Y.; Kinaret, J.; Garcia-Sanchez, D.; Bachtold, A. *Science* **2009**, *325*, 1107.
(8) Laird, E. A.; Pei, F.; Tang, W.; Steele, G. A.; Kouwenhoven, L. P. *Nano Lett.* **2012**, *12*, 193.
(9) Eichler, A.; Moser, J.; Chaste, J.; Zdrojek, M.; Wilson-Rae, I.; Bachtold, A. *Nat. Nanotechnol.* **2011**, *6*, 339.
(10) Poncharal, P.; Wang, Z. L.; Ugarte, D.; de Heer, W. A. *Science* **1999**, *283*, 1513.
(11) Jensen, K.; Kim, K. P.; Zettl, A. *Nat. Nanotechnol.* **2008**, *3*, 533.
(12) Lassagne, B.; Ugnati, D.; Respaud, M. *Phys. Rev. Lett.* **2011**, *107*, 130801.
(13) Hüttel, A. K.; Steele, G. A.; Witkamp, B.; Poot, M.; Kouwenhoven, L. P.; van der Zant, H. S. J. *Nano Lett.* **2009**, *9*, 2547.
(14) Wu, C. C.; Liu, C. H.; Zhong, Z. H. *Nano Lett.* **2010**, *10*, 1032.
(15) Jin, Z.; Chu, H. B.; Wang, J. Y.; Hong, J. X.; Tan, W. C.; Li, Y. *Nano Lett.* **2007**, *7*, 2073.
(16) Luo, J.; Warner, J. H.; Feng, C. Q.; Yao, Y. G.; Jin, Z.; Wang, H. L.; Pan, C. F.; Wang, S.; Yang, L. J.; Li, Y.; Zhang, J.; Watt, A. A. R.; Peng, L. −M.; Zhu, J.; Briggs, G. A. D. *Appl. Phys. Lett.* **2010**, *96*, 213113.
(17) Luo, J.; Tian, P.; Pan, C. −T.; Robertson, A. W.; Warner, J. H.; Hill, E. W.; Briggs, G. A. D. *ACS Nano* **2011**, *5*, 1047.
(18) Timoshenko, S. P.; Gere, J. M. *Theory of Elastic Stability*, 2nd ed.; Dove Publications: New York, 2009.
(19) Joy, D. C.; Joy, C. S. *Micron* **1996**, *27*, 247.
(20) Cazaux, J. *J. Appl. Phys.* **1986**, *59*, 1418.
(21) Lu, J. P. *Phys. Rev. Lett.* **1997**, *79*, 1297.
(22) Lee, S. Y.; Chao, J. C. *J. Sound Vib.* **2000**, *238*, 443.
(23) Markus, S.; Nanasi, T. *Shock Vib. Dig.* **1981**, *7*, 3.
(24) de Jonge, N.; Lamy, Y.; Schoots, K.; Oosterkamp, T. H. *Nature* **2002**, *420*, 393.
(25) Krüger, A.; Ozawa, M.; Banhart, F. *Appl. Phys. Lett.* **2003**, *83*, 5056.
(26) Dresselhaus, M. S.; Dresselhaus, G.; Jorio, A.; Souza Filho, A. G.; Saito, R. *Carbon* **2002**, *40*, 2043.